*Science and Technology*, 1 (1996) 55-61


# Cation Distribution in Natural Chromites from Oman

**Z. Al-Alawi, A.M. Gismelseed, A. A. Yousif, M. A. Worthing, H. H. Sutherland, A. M. Rais, M. E. Elzain and A. D. Al-Rawas**

*College of Science, Sultan Qaboos University, P.O.Box 36, Al-Khod 123, Muscat, Sultanate of Oman.*

خلاصة : تمت دراسة عينتين من الكروم الطبيعي المتواجد في الأفيوليت العمانية باستخدام مطياف الموسباور ، حيود الأشعة السينية والمجهر الالكتروني . نمط الحيود الذي قيس عند درجة حرارة الغرفة يدل على أن العينتين ذواتا تركيب مكعب سبانيل مركزي الوجه . حللت قياسات مطياف الموسباور للعينتين عند درجات حرارة ٢٩٥ ، ١٦٠ ، ٧٨ كلفن بإدخال ثلاثة أشكال ثنائية تدل اثنتان منها على وجود حديد ثنائي التكافؤ ($Fe^{2+}$) في مواقع رباعية الأسطح ($A_1$,$A_2$) والثالث يدل على وجود حديد ثلاثي التكافؤ ($Fe^{3}$) في مواقع ثماني الأسطح (B) . استخدمت نسبة الحديدوز/الحديديك المستنتج من مطياف الموسباور مع التركيز الذري المستخلص من معطيات المنظار الدقيق في استخلاص التركيبه الكيميائية للعينتين وهذه النتائج تؤيد نموذج توزيع الكاتيون .

ABSTRACT: Two specimens of natural chromite from the Oman ophiolite were studied using Mössbauer Spectroscopy (MS), X-ray Diffraction (XRD), and Scanning Electron Microscopy (SEM). The diffraction patterns obtained at room temperature showed that the two specimens have a face-centered cubic spinel structure. Their Mössbauer spectra at 295 K, 160 K and 78 K have been fitted to three doublets, assigned to two $Fe^{2+}$at the tetrahedral ($A_1$, $A_2$) sites and one $Fe^{3+}$ at the octahedral (B) site. The ferrous/ferric ratio obtained from the Mössbauer analysis together with the atomic concentration derived from the microprobe data are used to derive the chemical formulae for the two specimens. The data also supports a model of ordered cation distribution in the specimens examined.

Pure chromite is very rare in nature and, when developed naturally, it is commonly associated with different types of gangue. In ophiolite occurrences, the nature of the gangue varies from deep (mantle) to shallower (transition zone and stratiform) deposits. In deep deposits olivine predominates, whereas pyroxene accompanied by plagioclase become abundant in deposits at the top of the mantle. The nature of the gangue may give an indication of the depth of chromite formation.

Cations in chromite prefer to occupy one of the two non-equivalent available sites. The extent of the ordering depends on the type of constituent cations involved and conditions of formation such as temperature and pressure and the cooling history of the sample (Bancroft 1973). The degree of ordering, and thus the cation distribution, is expected to be different in minerals formed under igneous conditions to that formed under metamorphic conditions.

Valuable geothermometric data may be obtained from measurements of the cation distribution of natural chromites. Such geothermometers can be calibrated by experimental synthesis of chromite under different pressure and temperature conditions.

Natural chromites have a wide range of chemical composition. There have been conflicting reports on the distribution of cations on the tetrahedral and octahedral sites. Mössbauer data on natural chromites have been interpreted to indicate a disordered distribution of reported electron transfer between $Fe^{2+}$ and $Fe^{3+}$ (Da Silva *et al*, 1975; Fatseas *et al*, 1976). The latter authors have also reported electron transfer between $Fe^{2+}$ and $Fe^{3+}$ of crystallographically identical sites. On the other hand, a detailed Mössbauer investigation on synthetic and natural chromite has been interpreted as an ordered arrangement of the normal spinel structure (Osborne *et al*, 1981, Bancroft *et al*, 1983). No evidence of disorder or electron delocalization effects has been observed. We have used Mössbauer, X-ray diffraction and scanning electron microscopy to investigate natural chromites from the Oman ophiolite. The interpretation of our data supports the model of an ordered distribution of cations.

## Geological Aspects

Chromite is a common accessory mineral in many mafic and ultramafic igneous rocks but its modal abundance depends on a number of factors including oxygen fugacity and the availability of chromium in the crystallising magma. Under the right physiochemical conditions, chromite may be an abundant cumulus mineral in mafic magmas and may be concentrated into workable ore deposits by gravity settling in magma chambers. For example, in layered mafic intrusions such as the Bushveld Complex of South Africa, chromite layers

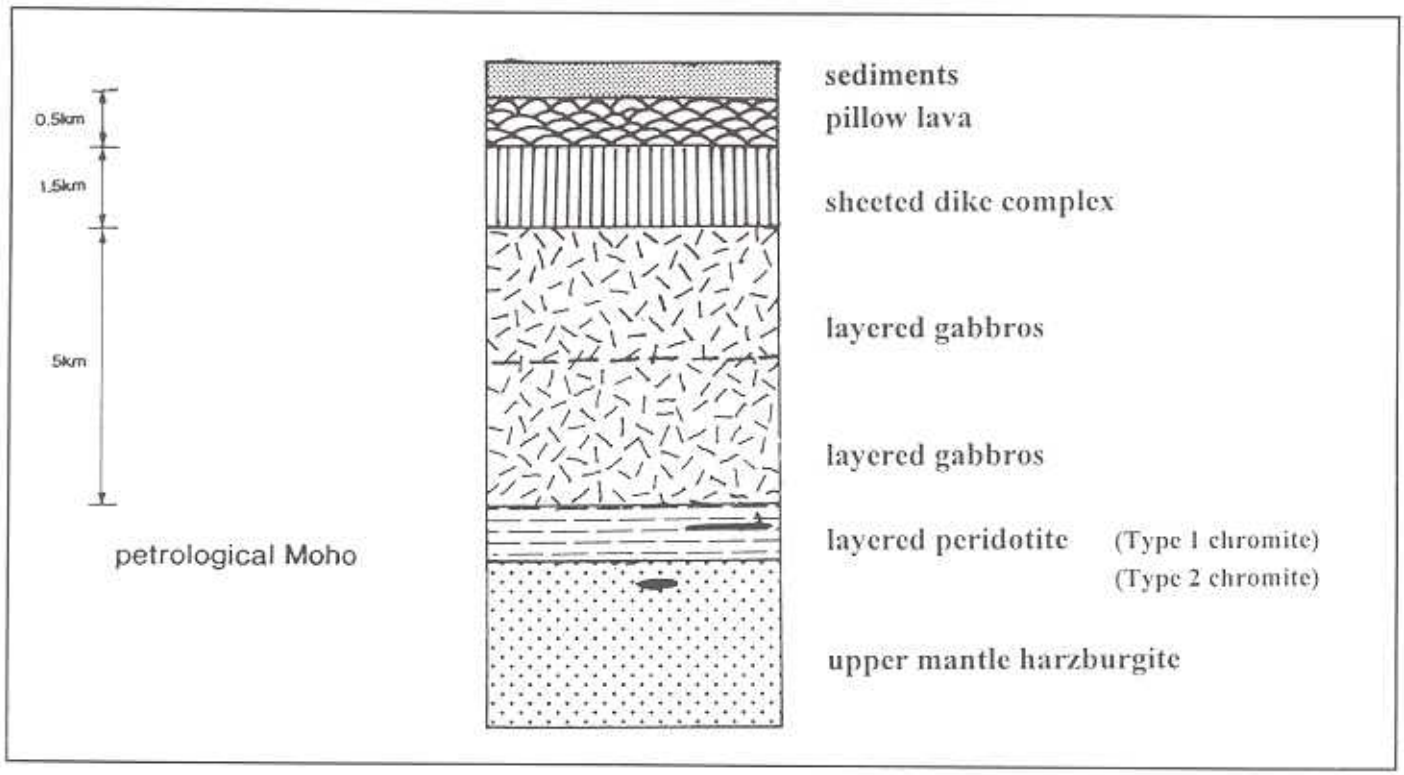


**Figure 1.** Schematic cross-section through the Oman ophiolite showing main rock type and the stratigraphic position of the two types of chromites.

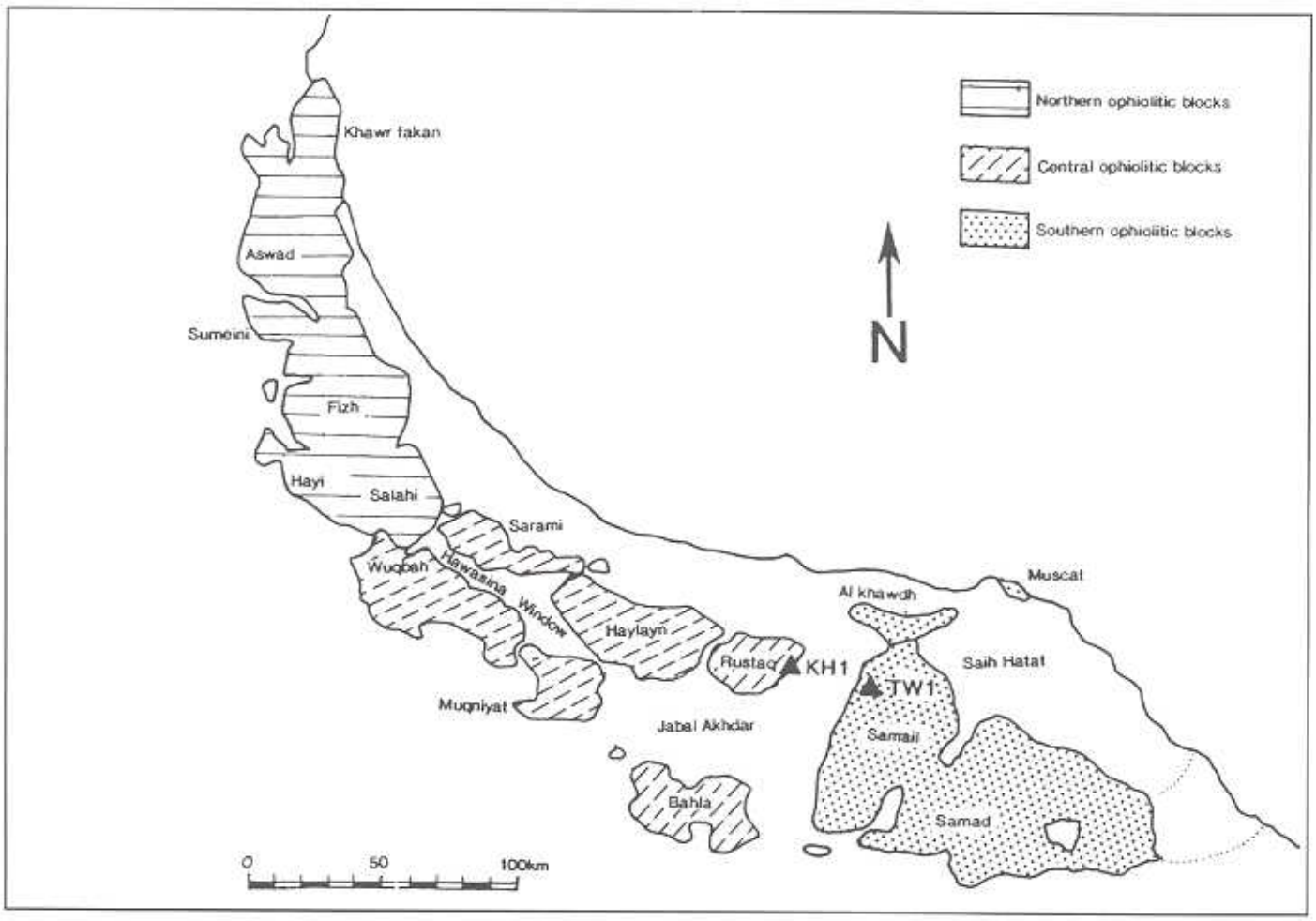


**Figure 2.** Map of Northern Oman showing ophiolite outcrop. The position of the two chromite samples is also shown.

up to two meters thick can be traced laterally for 60 kilometers and form the world's richest source of chromium (Evans, 1987).

In Oman, chromite is found in economic concentrations in the Samail ophiolite (Batchelor, 1992). The ophiolite is a slab of oceanic crust and mantle that was obducted onto the Arabian Platform in late Cretaceous times. The simplified structure of the Samail ophiolite is shown in Figure 1. The lower unit of the sequence is part of the earth's upper mantle and is separated from the overlying crustal sequence by the petrological moho. It comprises a thick sequence of ultramafic rocks known as harzburgites which represent the residue left after basaltic magma has been extracted by partial melting.

Pods and bands of chromite occur most commonly in the upper 500 meters of the mantle sequence where they are usually associated with dunite. These are the Type 2 podiform deposits of Batchelor (1992).

The lower part of the crustal sequence represents a magma chamber which contained magma derived from the partially melted mantle underneath. This sequence begins with cumulus ultramafic rocks formed by gravity settling of early formed minerals such as chromite, olivine and pyroxene. The chromite in these rocks thus occurs as layers rather than pods; the Type 1 stratiform deposits of Batchelor (1992).

The cumulus ultramafics grade upwards into a thick sequence of layered gabbros which crystallised by gravity settling in a magma chamber periodically replenished with fresh magma from below. The gabbros are overlain by a sheeted dyke complex. These subvertical intrusions represent the conduits which fed magma from the underlying magma chamber up to the submarine surface above. The top of the ophiolite is represented by a thick sequence of pillow basalts which formed by rapid chilling of hot basaltic magma as it came into contact with cold sea water.

The Samail ophiolite is an example of the harzburgite ophiolite type (HOT), so called because the mantle sequence is dominated by the depleted ultramafic rock known as harzburgite. This ophiolite type is believed to form at fast spreading oceanic ridges (Nicholas and Azri, 1991). In this tectonic environment a high rate of magma production is required to feed the high spreading rate. Thus chromium, which at slow spreading ridges, remains partitioned in unmelted mantle clinopyroxene, passes into basaltic magma by partial melting. According to the model of Cassard (1981), this magma rises along conduits in the mantle towards the overlying magma chamber simultaneously crystallising chromite. The dense chromite crystals are winnowed out of the ascending magma in places where the conduits widen, thus forming vertical or sub-vertical accumulations of podiform chromite.

These deposits are subsequently rotated and streaked out into horizontal or sub-horizontal pods by the pervasive lateral flow that characterizes the mantle under spreading ridges (Cassard 1981). Both samples studied in this paper are from Type 2 podiform deposits.

## Experimental

The samples were collected from the Al-Tawiyah chromite deposit (KH1) which is some 15 km NNW of Nakhal and from Khobar (TW1) on the Luzugh-Samail Road (Fig. 2). Both are classified as Type 2 podiform chromites.

Magnetic separation and washing were used to separate the chromite from the gangue. The samples were sieved to get rid of the fine fraction and grains with sizes of 335 $\mu$m were passed through the magnetic separator. The process was repeated several times and each time the chromite and gangue were checked under the binocular microscope to verify good separation. About 90% TW1 pure chromite resulted from magnetic separation and less than 5% of the raw material was lost, but more impurities were detected in the KH1 resulting in a separated portion of about 70%. Moreover, while TW1 shows one type of gangue, KH1 shows two distinct impurities. The chromite obtained from the magnetic separator was then washed several times with distilled water and allowed to dry at ambient temperature. The washing process removed about 1% of the residual impurities.

Polished thin sections (30 $\mu$m thick) of chromite were prepared for the optical microscope and scanning electron microscope. The samples were analysed on a Jeol JSM 840A SEM with Link AN10/85S energy dispersive X-ray microanalyser. Operating conditions included an accelerating voltage of 20 kV, current 1 nA and a livetime of 100 seconds. A number of traverses were made across individual chromite grains to test for zoning, none was found. Further analyses were then performed randomly throughout the slide.

Powdered specimens were prepared for the X-ray diffraction (XRD) and Mössbauer studies. The X-ray data were collected using a Philips PW1820 vertical goniometer with monochromator and automatic divergence slit attached to a PW1700 generator operating at a voltage of 40 kV, current of 40 mA and controlled by a micro PDP11 computer. Scans in the 2 - 140° 2$\theta$ range were obtained using a step size of 0.02°, sample time of 2s and $CuK_\alpha$ radiation. The peak positions were identified using the Philips APD peak search program and the JCPDS files helped in the identification.

Mössbauer spectra were obtained using a $^{57}$CoRh source and a spectrometer in the constant acceleration mode. Measurements at temperatures of 78, 160 and 295K were performed with a liquid flow cryostat. Least square fitting techniques were used for the analyses of the data and $\alpha$-Fe for the calibration of the spectrometer.

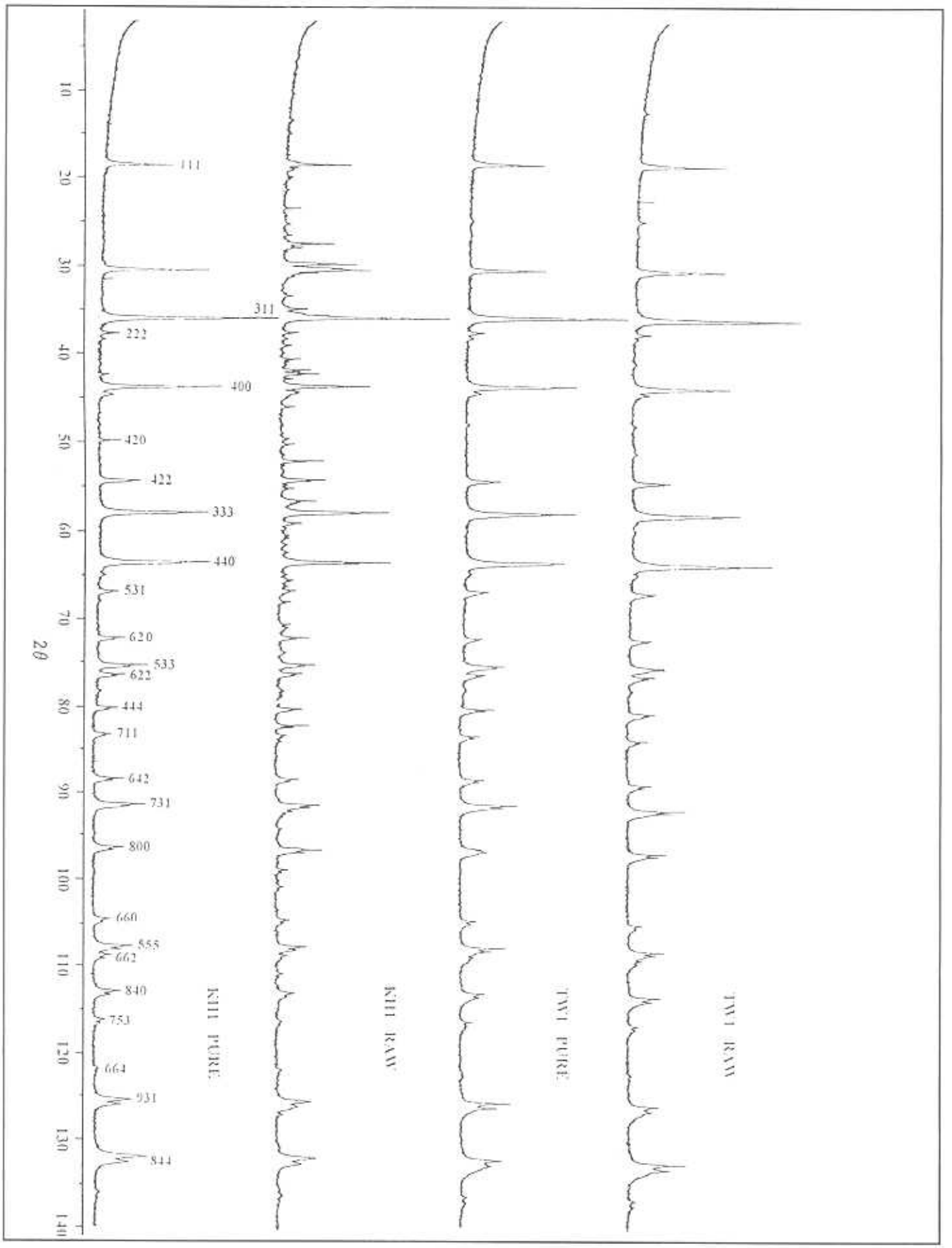


**Figure 3.** X-ray diffraction patterns of TW1 and KH1 chromites scanned from 2°-240° 2θ. The TW1 raw chromite contains dolomite as an impurity and the KH1 raw chromite contains augite and thomsonite with some plagioclase.

## Results

The chromite samples consist of Fe, Al, Mg in addition to Cr as major components. Traces of Ti and Mn (< 0.01 at %) were also detected but have been neglected in establishing the chemical formulae. The average atom concentration for TW1 and KH1 samples as obtained from the SEM semi-quantitative analysis are given in Table 1.

The X-ray diffraction patterns of the raw and separated specimens verified the efficiency of separation as shown in Figure 3, and the JCPDS files were used to identify the impurities in each specimen. The impurity in the TW1 is dolomite. In KH1, augite, a type of pyroxene commonly associated with chromite, and thomsonite, which belongs to the zeolite group, were detected. There is a small amount of plagioclase in the thomsonite specimen, which suggests that the former has been altered to the latter. The diffraction patterns of the pure specimens showed that TW1 and KH1 have a face-centered cubic spinel structure at room temperature, giving low angle reflections from the planes (111), (220), (311), (222), (400), (420), (422), (333) and (440). The *d* spacings were calculated and lattice parameters extracted from the reflection planes. These parameters were fitted using the extrapolation function $F(\theta) = \frac{1}{2}(\cos^2\theta/\sin\theta + \cos^2\theta/\theta)$. The result of the fit gave lattice parameters of 8.246(3) and 8.265(3) Å for TW1 and KH1 respectively.

The Mössbauer spectra of TW1 and KH1 at 78, 160K and room temperature show similar paramagnetic patterns. Figure 4 shows representative spectra. The spectra were fitted with three doublets that gave consistent parameters for the three temperatures. Table 2 presents some of the Mössbauer parameters.

## Discussion

The assignment of the iron cations to the octahedral and tetrahedral sites has been achieved using the Mössbauer parameters (Bancroft 1973; and Osborne *et al*, 1981). A ferric cation resides on the B-site ($Fe^{3+}_{B}$) and two ferrous cations sit on the tetrahedral sites ($Fe^{2+}_{A1}$ and $Fe^{2+}_{A2}$). The linewidths of the Lorentzian lines vary between 0.4 and 0.5 mms $^{-1}$. The increased linewidth and similarity of isomer shifts of the two A-sites suggest a distribution of parameters as a result of different surroundings.

TABLE 1

*The average atom concentration for TW1 and KH1 as obtained from the qualitative analysis of the SEM.*

| ATOM TYPE | TW1 ± 0.01 | KH1 ± 0.01 |
|---|---|---|
| Mg | 0.80 | 0.71 |
| Fe | 0.23 | 0.41 |
| Al | 0.93 | 0.89 |
| Cr | 1.03 | 0.99 |

TABLE 2

*Mössbauer parameters of TW1 and KH1 Oman ophiolites. $A_1$ and $A_2$ refer to the tetrahedral cation sites and B to the octahedral cation site; isomer shifts δ are relative to α-Fe.*

| | | Site $A_1$ | | | Site $A_2$ | | | Site B | | |
|---|---|---|---|---|---|---|---|---|---|---|
| | Temperature | δ±.03 | ΔEQ±.02 | A%±.3 | δ±.03 | ΔEQ±.02 | A%±.3 | δ±.03 | ΔEQ±.02 | A%±.3 |
| Sample | T K | mm/s | mm/s | | mm/s | mm/s | | mm/s | mm/s | |
| | 78 | 1.13 | 2.80 | 39.2 | 1.21 | 1.93 | 20.6 | 0.45 | 0.71 | 40.2 |
| TW1 | 160 | 0.98 | 2.52 | 39.9 | 1.03 | 1.46 | 20.0 | 0.39 | 0.66 | 40.1 |
| | 295 | 0.75 | 1.93 | 40.0 | 0.87 | 0.90 | 20.0 | 0.30 | 0.55 | 40.0 |
| | 78 | 1.05 | 2.92 | 50.6 | 1.19 | 1.93 | 19.0 | 0.39 | 0.68 | 30.4 |
| KH1 | 160 | 1.00 | 2.42 | 50.2 | 1.00 | 1.49 | 19.2 | 0.35 | 0.63 | 30.6 |
| | 295 | 0.81 | 1.82 | 50.9 | 0.84 | 0.98 | 19.6 | 0.26 | 0.53 | 29.5 |

However, a good fit is obtained on fitting the spectra with two sites. In this fit the second A-site was clearly identified with a quadrupole splitting that differs from the first one by 45% and 51% for TW1 and KH1 respectively. Moreover, we observe a different temperature dependence of δ and $\Delta E$ for the two sites. Using the 78 K and room temperature data for TW1, we observe a reduction in isomer shift of 34% and 28%,and in quadrupole splitting of 31% for A1 and A2 respectively. We also observe that while δ and $\Delta E$ and their temperature dependence for sites B and A2 in the two samples are similar within the experimental error, those for site A1 differ markedly. A similar interpretation of two A-sites has been reported recently for data on natural chromites from China and been attributed to next nearest effects where a particular configuration exists for each site (Chen and Chen, 1992). This has also been supported by reports of the appearance of a peak in substitution of Rh/In and Fe for Cr in the ordered synthetic spinels $FeCr_2S_4$ and $FeCr_2O_4$ . While the centre shifts in these spectra remain the same, the quadrupole splitting changed markedly with substitution (Robbins *et al*, 19971; Riedel and Karl, 1980 and 1981). The area ratio of the three sites remains the same at the different temperatures within the experimental error. This suggests equal f-factors at the tetrahedral and octahedral sites and the population of iron cations in TW1 and KH1 in each site was taken from the area ratios. Swatzky *et al* (1969) obtained a ratio of 0.94 for $f_B/f_{A4}$ in $Fe_3O_4$, which indicate a larger f-factor for the tetrahedral sites in the magnetite.

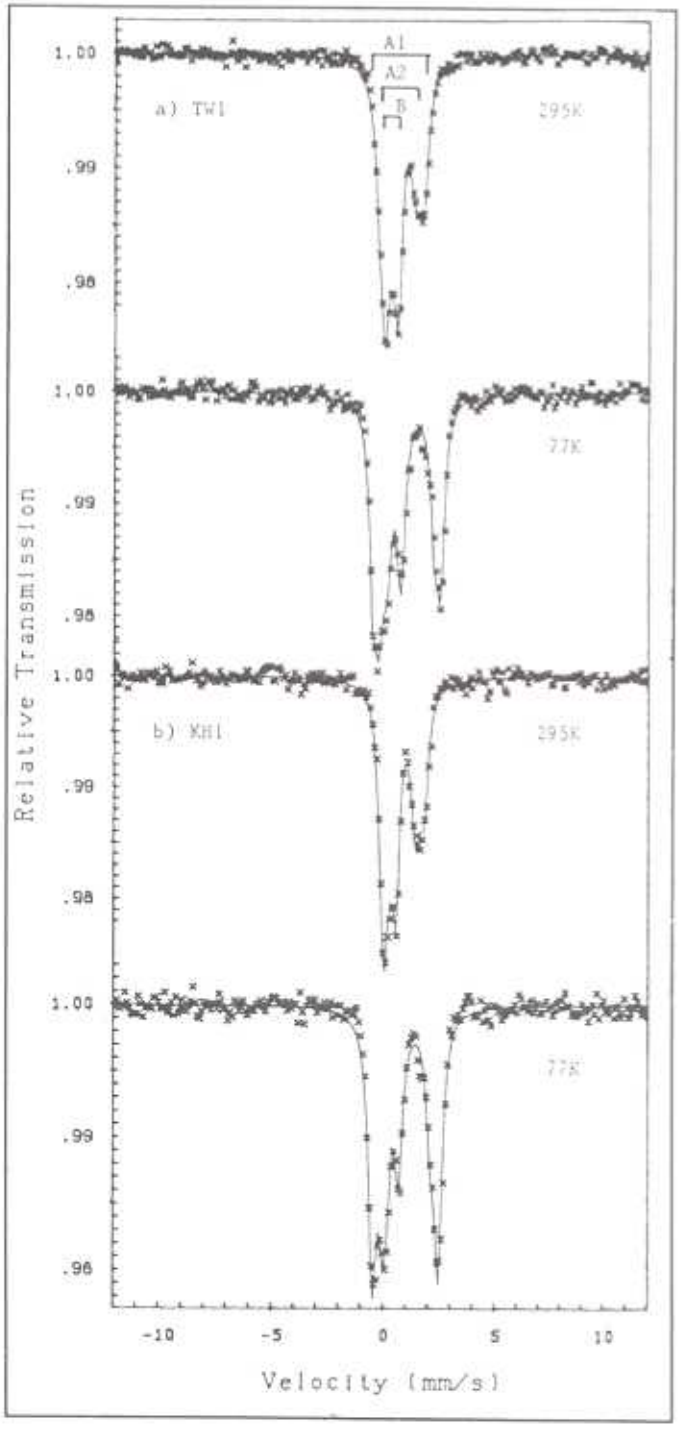


**Figure 4.** Mössbauer spectra of (a) TW1 and (b) KH1 taken at 295 K and 77 K, and fitted with the parameters listed in Table 2.

We have used the atomic concentrations derived from the SEM microanalyser and the ferrous/ferric ratio obtained from the Mossbauer analyses, to derive the chemical formulae for the two ferrites. With $Mg^{2+}$ occupying the tetrahedral sites and $Cr^{3+}$ in the octahedral sites (Fatseas *et al*, 1979; Chen and Chen, 1992), it would be possible to propose chemical formulae with detailed cation-distributions at room temperature for the TW1 and KH1 respectively as follows:

$$(Fe^{2+}_{0.14}Mg^{2+}_{0.80}Al^{3+}_{0.06})^A\ [Fe^{3+}_{0.09}Cr^{3+}_{1.03}Al^{3+}_{0.87}]^B\ O_{3.99}$$

$$(Fe^{2+}_{0.29}Mg^{2+}_{0.71})^A\ [Fe^{3+}_{0.12}Cr^{3+}_{0.99}Al^{3+}_{0.89}]^B\ O_4$$

The rest of the tetrahedral sites in TW1 have been filled with $Al^{3+}$. The site occupancy of aluminium in ferrites has also received some discussion. Studies on aluminous magnetites have been interpreted with $Al^{3+}$ occuping the octahedral sites only (Pickart and Turnock, 1959), or to have a B-site preference (Navrotsky and Kleppa, 1967; Kulshrestha and Ritter 1985). We have shown in an investigation on $Cl(Al,Fe)_2O_4$ that Al can occupy tetrahedral sites (Yousif *et al*, 1991). Osborne *et al* (1981) and Bancroft *et al* (1983) have studied $Fe(Cr,Al)_2O_4$ and natural chromites, but observed no evidence of any tetrahedral $Al^{3+}$. However, Fatseas *et al* (1979) have established chemical formulae for natural chromites with up to 0.22 % Al occupying the tetrahedral sites. A stronger preference of $Al^{3+}$ on the A-sites than either of $Fe^{3+}$ or $Cr^{3+}$ is assumed here.

The lattice constants of TW1 and KH1 are smaller than that of synthetic chromite of 8.337 Å (Blasse, 1964). Moreover, there is a clear variation in lattice parameters of the two chromites which is due to the influence of the size of substituent cations. A bigger component of the

size of substituent cations. A bigger component of the large divalent iron in KH1 as opposed to that of the smaller trivalent aluminium in TW1 is responsible for the larger lattice constant in the former component. We have used the lattice parameters and published ionic radii to estimate the oxygen parameter which is a measure of deviation of the spinel from an ideal structure. The following values: $r_1 = 0.66$ Å, $r_2 = 0.74$ Å, $r_3 = 0.64$ Å, $r_4 = 0.51$ Å, $r_5 = 0.63$ Å and $r_o = 1.32$ Å were used for the ionic radii of $Mg^{2+}$, $Fe^{2+}$, $Fe^{3+}$, $Al^{3+}$, $Cr^{3+}$ and $O^{2-}$ ions respectively (Weast and Astle, 1983). The average cation radii $r_A$ and $r_B$ of the A-site and B-site for TW1 and KH1 were calculated using the weights of various cations in each site. These are also related to the lattice parameter, $a$, oxygen parameter, $u$, and the oxygen anion radius, $r_o$ through (Standley, 1972):

$$r_A = (u - 0.25)\sqrt{3}\, a - r_o$$
$$r_B = (0.625 - u)\, a - r_o$$

An oxygen parameter $u = 0.392$ (2) for both samples was calculated, which is much higher than the ideal structure value of 0.375. A higher anion parameter implies larger A-sites. Since each anion ($O^{2-}$) in the spinel structure is surrounded by one A and 3B cations, regarding the spinel unit cell, the cation-oxygen bond length for the A-sites and B-sites were calculated. The former bond length was found to be larger by 5.5% for both spinels. This may have softened the phonon spectrum at the A-sites, which results in a smaller f-factor producing a higher $f_B / f_A$ than that reported for similar minerals.

## Conclusion

Two chromite samples were collected from Al Tawiyah (KH1) and Khobar (TW1). Both samples are Type 2 chromite from the upper part of the mantle sequence of the Oman opiolites.

The derived chemical formulae for the two samples show that in addition to Cr they contain Fe, Al and Mg. These results support the consistency of Mössbauer parameters which suggest the presence of identical sites in the two samples. The ferrous/ferric ratio remains constant at different temperatures which supports an ordered distribution of the cations.

## References


BANCROFT G. M., 1973. *Mössbauer Spectroscopy: An Introduction to Inorganic Chemists and Geochemists* McGraw-Hill, England.

BANCROFT G. M., M. D. Osborne and M. E. Fleet, 1976. *Solid State Communication* **47** (8), 623.

BLASSE G., 1964. *Philips Res.* **17**, 68.

BACHELOR D. A. F., 1992. *Transactions of the Institute of Mining and Metallurgy*, **101**, B108-B230.

CASSARD D., A. NICOLAS, M. RABINOWICZ, M. MOUTTE, M. LEBLANC, A. PRINZHOFER, 1981. *Teco. Geol.* **76**, 805-831.

CHEN Y. L., B. B. XU. and J. G. CHEN, 1976. *Hyp. Int* **70**, 1029.

DA SILVA E. G., A. ABRAS and A. O. R. SETTE CAMARA, 1976. *J.Phys.* **12**, 783.

EVANS A. M., 1987. *An Introduction to Ore Geology* (Blackwell, Oxford, U.K..

FATSEAS G. A., J. L. DORMAN, and H. BLANCHARD, 1976. *J. Phys.* **12**, 787.

KULSHRESTHA S. K. and G. RITTER, J. 1985. *Mater. Sci.* **20**, 821.

NAVROTSKY A. and O. J. KIEPPA, 1967. *J. Inorgan Nucl Chem* **29**, 2701.

NICOLAS A. and H. Al-AZRI, Chromite-rich and Chromite-Poor Ophiolites: The Oman Case in Ophiolite Genesis and Evolution of the Oceanic Lithosphere. Eds. T. J. Peters, A. Nicolas and R. G. Coleman, Kluwer Academic Publishers, Dordrecht, Netherlands, pp 261-274 (1991).

OSBORNE M. D., M. E. FLEET, and G. M. BANCROFT, 1981. Contrib. Mineral Petrol. 77, 251.

PICKET S. J. and TURNOCK,1959. *J. Phys. Chem. Solids* **10**, 242.

RIEDEL E. and R. KARL, 1980. *J. Solid State Chem.* **35**, 77.

RIEDEL E. and R. KARL, 1981. *J. Solid State Chem.* **38**, 40.

ROBBINS M., G. K. WERTHEIM, R. C. SHERWOOD, and D. N. E. BUCHANAN, 1971. *J Phys. Chem. Solids* **32**, 717.

STANDLEY K. J., 1972. *Oxide Magnetic Materials*, p26-27, (Clarendon, Oxford).

SWATZKY G. A., VAN DER WONDE, and A. H. MORRISH, 1969. *Phys. Rev.***183**, 383.

WEAST R. C. and M. J. ASTLE (Eds.), *1983. CRC Handbook of Chemistry and Physics*, 63rd Edition, CRC Press.

YOUSIF A. A., M. E. ELZAIN, H. H. SUTHERLAND, and S. H. SALAH, 1991. *Hyp. Int.* **68**, 323.



Received 8 January 1996
Accepted 11 June 1996